

Shape optimization of a multi-element hydrofoil for hydrokinetic turbines using response surface methodology

Rubio-Clemente A^{1,2}., Aguilar J²., Chica E²

¹ Facultad de Ingeniería, Tecnológico de Antioquia–Institución Universitaria TdeA, Calle 78b, No. 72A-220, Medellín, Colombia.

² Departamento de Ingeniería Mecánica, Facultad de Ingeniería, Universidad de Antioquia UdeA, Calle 70, No. 52-21, Medellín, Colombia.

Phone/Fax number: +0057 2195547, e-mail: ainhoarubioclem@gmail.com

Abstract. This paper describes the optimization procedure of a two-dimensional multi-element hydrofoil shape during its design for small horizontal axis hydrokinetic turbines using response surface methodology. JavaFoil software was used for describing the hydrofoil performance under several combinations of geometrical parameters, such as the horizontal space (overlap), h , between the drag edge of the main element and the leading edge of the second element; the vertical distance (gap), d , of the flap from the main element trailing edge; and the flap deflection angle, δ . Different experimental designs aiming at the maximization of the lift-to-drag ratio were used. The maximal lift-to-drag ratio was found to be 69.9626 for d , h and δ equal to 2.0%, 18.4619% and 20°, respectively, being δ the factor exerting a considerable influence on the response variable.

Key words. Hydrokinetic turbine, hydrofoil optimization, response surface methodology, design of experiments

1. Introduction

Today, the growth of conventional hydropower plants is constrained by the number of available natural sites, large capital (initial) investment, extensive pay-back time, and environmental concerns [1], [2]. As a matter of fact, flooding land for a hydroelectric reservoir performance has an extreme environmental impact since it is involved in the destruction of forest, wildlife habitat and agricultural land, among other detrimental effects on the environment [1], [3]. Even in many instances, entire communities are required to be relocated to make way for man-made reservoirs [1-3].

Nowadays, hydrokinetic systems offer many advantages compared to other sources of electrical energy production, especially compared to hydropower plants, as hydrokinetic systems are portable systems with small initial set-up costs, do not require large infrastructure and can be quickly deployed [1], [2]. Hydrokinetic systems employ a hydrokinetic turbine which utilizes the kinetic energy of flowing water for power generation [1]-[3]. From the viewpoint of engineering design, the more torque has the turbine rotor, the more power will be developed. Consequently, the generation of the maximal possible torque and turbine rotor velocity is desired at the design stage of a hydrokinetic system [1]-[3]. Torque and angular velocity of the rotor are achieved by hydrofoil lift forces. It must be taken into account that lift force depends of the change of pressure generated in the hydrofoil surface [2]-[3]. This pressure depends on various parameters, like fluid density, number or blades, tip speed ratio and hydrofoil profile shape (angle of attack, blade pitch, chord length and twist and its distribution along the blade span) [1-3].

The parameters within a hydrokinetic turbine that designers seek to optimize have evolved in recent years [3], [4]. However, in general, efforts are focused on the maximization of the power coefficient, C_p , *i.e.*, the fraction of power in water that can be extracted by the hydrokinetic turbine [4]. The optimization strategy has a direct impact on the blade shape due to the hydrofoil shape contributes to the generation of a lift coefficient by creating suction on the hydrofoil upper surface [4], [5]. During this process, a drag is also generated, which is not desirable for the maximization of the power output of the hydrokinetic turbine [1]-[3]. To get the maximum torque and power output from the hydrokinetic turbine, having a hydrofoil generating high lift and high lift-to-drag ratio is of crucial interest [2], [3]. Therefore, for the selection of a proper turbine hydrofoil is very important at the initial stage of the design process. Nowadays, multi-element hydrofoils or high-lift systems have been proposed as an alternative concept allowing improving the blade performance [5]. In fact, in the literature there are few publications that consider multi-element hydrofoil in hydrokinetic turbines design [6]. From the authors' knowledge, there is only one work considering the use of a double-blade hydrofoil for generating the maximum lift [7]. However, several numerical studies on multi-element airfoil configurations for wind turbines have been reported [8]-[10].

A multi-element profile can be conformed of 3 or 2 elements, a main profile and 1 or 2 flaps [8]-[10]. The variables involved in the geometrical design of a multi-element hydrofoil are the chord length, c ; the main element chord length, c_1 ; the flap chord length, c_2 ; the angle of attack, α ; the gap size, d , defined as the minimal vertical distance of the flap from the main element trailing edge; the overlap distance, h , which refers to the distance of the flap leading edge from the main element trailing edge along the main element chord; and the flap deflection angle, δ [8]-[10].

Several strategies have been proposed to optimize the parameters involved in the blade design, being response surface methodology (RSM) widely used in the aerodynamic optimization of airfoils [11]-[14]. RSM is defined as a collection of statistical and mathematical methods useful for developing and improving the optimization of a process, which uses collectively design of experiments (DOE), analysis of variance (ANOVA) and regression analysis. The methodology is a general approach to describe the behavior of certain output variables, known as response factors, towards the change of independent parameters, so-called independent factors; that is, the influencing variables [15]. For a well distributed number of design points in the space of the independent variables, a regression function; *i.e.*, an objective function, is created through the least-square approach, which in turn can be used as the basis for different optimization purposes [15].

Thus, the current study is focused on the hydrodynamic optimization of several two-dimensional configurations of a multi-element hydrofoil for high lift applications. For this purpose, RSM is used to build a functional relationship between the influencing variables (d , h , and δ) and the desired objective function; *i.e.*, the lift-to-drag ratio. This ratio was maximized to obtain the highest power achieving a stable operation within the water current.

Thus, this work enables for the first time to optimize the geometrical parameters of a multi-element hydrofoil for hydrokinetic turbine application.

2. Methods and materials

2.1 Hydrofoil characteristics

High-lift systems have been designed in aircraft applications with the objective of achieving high levels of performance while maintaining the flow attached on the single-segment flap [8]-[10]. Due to there is a continuous need to improve the lift and lift-to-drag ratio of the hydrofoil for turbine application, the concept of multi-element hydrofoil can be used for the blade design of hydrokinetic turbines. A typical multi-element hydrofoil often consists of a main element with a leading-edge slat and trailing-edge flap elements that can be hydrodynamically highly efficient. However, a complex structure and an expensive design and maintenance costs are required [8]-[10]. Additionally, because of the interaction among each of its components and parts, the flow field around a multi-element hydrofoil has very complicated physics, which are significantly influenced by the change in the distance between such as components and their h and δ [16].

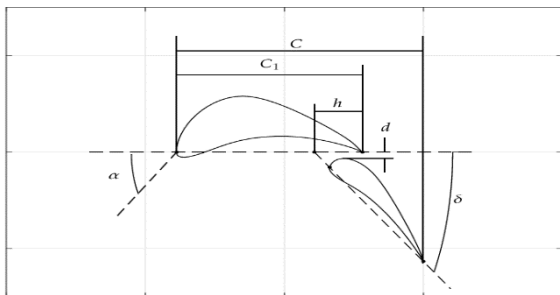


Figure 1. Schema of the multi-element hydrofoil

In the present study, the Eppler 420 airfoil was used as the hydrofoil cross section (Figure 1). Furthermore, utilizing JavaFoil code, the profile was analyzed using different α , h , d and δ , in order to compute the hydrodynamic performance, such as the lift coefficient, C_L , versus α , and the drag coefficient, C_D , versus C_L . Moreover, d was increased from 2%-chord to 4%-chord; h was increased from 5%-chord to 20%-chord and δ was increased from 20° to 40° . In order to reduce the number of design variables, α was fixed at 0° for a Reynolds number of 7.5×10^5 .

3. Response surface methodology

Response surface methodology (RSM) is used to approximate functional relationships between a response variable, y , and a set of design variables, x , which can be used to find the combination of factor levels for which the response variable is optimized [15]. In this context, the term “optimized” refers to either “maximize” or “minimize” [17]. It is highlighted that the primary advantage of RSM is the number of experimental treatment combinations and simulations required to find the optimal conditions which are reduced compared to the total number of treatment combinations used without utilizing RSM [18].

On the other hand, the choice of the DOE to be used in each particular case can have a large influence on the accuracy of the

approximation and the cost of constructing the response surface associated. Different DOE can be used, such as full factorial design, fractional factorial design, central composite design (CCD), Plackett-Burman, Doehlert designs, Taguchi method and Box-Behnken design (BBD), among other DOE [18].

The design procedure of RSM is as follows: 1) designing a series of experiments for an adequate and reliable measurement of the response of interest; 2) developing a mathematical model to construct the response surface containing the best fittings; 3) finding the optimal set of experimental parameters and levels that produces a maximal or minimal value of the response variable, depending on the goal set previously according to the process to be optimized, 4) representing the direct and interactive effects of the parameters influencing the system through two- and three-dimensional plots [15].

Under this scenario, the effect of different geometrical factors on the performance of a multi-element hydrofoil was investigated using a 3-level 3-factor full factorial experimental design, a BBD and a CCD. The list of the independent variables (x_1 , x_2 , x_3) with their codes and actual levels are presented in Table 1. The factor variables were studied and varied within 3 levels a) a high level, represented as (+1); b) a low level, referred as (-1); and c) a middle point, expressed as (0). The response variable, represented as y , was the lift-to-drag ratio. This response was intended to be maximized.

Table 1. Experimental range and levels of independent geometrical variables used during optimization procedures of the lift-to-drag ratio for a multi-element hydrofoil

Independent variable	Real values of coded levels			Symbol
	-1	0	+1	
Gap, d	2%-chord	3%-chord	4%-chord	x_1
Overlap, h	5%-chord	12.5%-chord	20%-chord	x_2
Flap deflection angle, δ	20°	30°	40°	x_3

-1: Factor at low level; 0: Factor at medium level; +1: Factor at high level

A second order polynomial equation was chosen to fit the experimental results. This model represents the main effects of geometrical variables (x_1 , x_2 , x_3) and their interactions on the response variable (C_L/C_D). The general form of the second order regression model chosen is represented by Equation (1).

$$y = \beta_0 + \beta_1 x_1 + \beta_2 x_2 + \beta_3 x_3 + \beta_{12} x_1 x_2 + \beta_{13} x_1 x_3 + \beta_{23} x_2 x_3 + \beta_{11} x_1^2 + \beta_{22} x_2^2 + \beta_{33} x_3^2 \quad (1)$$

where, y is the predicted response, β_0 is a constant value of the regression model; β_1 , β_2 and β_3 are linear coefficients, corresponding to the main effects; β_{12} , β_{13} and β_{23} are cross product coefficients, which represent the coefficient for the interaction effects. Finally, β_{11} , β_{22} and β_{33} are the quadratic coefficients. It is worth noting that a factor with a small individual or main effect can contribute greatly to the response by interacting with another one [16]-[18].

The contribution of each term in the regression and the significance of the model equations can be obtained through a fit test, known as ANOVA. This test is done by analyzing the magnitude of the sum of squares (SS), mean squares (MS), the Fischer test (F-test) and the lack-of-fit test (LOF) [15]-[18]. The sum of squares (SS) is a measurement of variability, and can be used to estimate the variance of the mean value of a statistical analysis when scaled for the degrees of freedom (df). In turn, the F-test of a model evaluates its significance by calculating the ratio between the regression MS and the residual MS. A small F-value of the regression model is not desired since it indicates that the variance is caused by random unexplained disturbances referred to as “noise” [15]-[18]. Additionally, p-value provides an indication of the significance of a model in relation with F-value. When p-value > F-value and p-value is lower than 0.05, the regression model is considered to be significant; therefore, the regression model built is able to explain the behavior of the studied factor variables, since the

chances that F-value is due to noise are < 5%. If p-value > F-value and it is above 0.05, the regression model constructed is insignificant; *i.e.*, it is not useful to explain the variability of the data obtained under the experimental domain considered [15]-[18].

In turn, LOF determines the inability of a model to fit experimental data that are not represented in the experimental domain. This is commonly done by calculating its F-value. A small F-value for the LOF is desired, since the experimenter look for the model to fit experimental or simulated data. When p-value > F-value and it is greater than 0.05, the LOF for the model is insignificant and the model is able to fit any data that are not specified in the experimental domain [15]-[18]. Nonetheless, it must be noted that a desired LOF does not guarantee the adequacy of a model; as a consequence, the coefficient of determination (R^2) must be also considered, given the fact that it measures the overall performance of the regression model built [15]-[18]. R^2 provides the summary statistic that measures how well the regression expression fits the data. Therefore, R^2 is expected to be as close to 1.0 as possible [15].

4. Results and discussion

3.1 3^3 Full factorial design

Full factorial DOE is probably the most common and intuitive strategy in DOE [15]. Therefore, the analyses of the obtained data were done using a standard full factorial (Table 2). This DOE represents the entire set of possible combinations among the levels of the factors run in a randomized sequence in order to meet the statistical requirement for independence of the observations [15]. For this purpose, each combination of the factor levels, known as treatments, was numerically processed using JavaFoil software. According to the DOE selected, 27 studies were carried out and a second-order polynomial regression model was developed using the numerical results.

Table 2. 3^3 Full factorial design matrix and responses

Run	Variables			Lift-to-drag ratio		% Error
	Gap, d (x_1)	Overlap, h (x_2)	Flap deflection angle, δ (x_3)	Numerical results	Predicted results	
1	3.0	20.0	30.0	56.7923	52.8070	7.02
2	2.0	12.5	30.0	46.1229	54.1188	-17.34
3	3.0	5.0	30.0	57.1184	48.8194	14.53
4	2.0	20.0	30.0	56.6672	49.4835	12.68
5	4.0	20.0	40.0	39.0216	39.6493	-1.61
6	3.0	20.0	40.0	38.4138	41.0229	-6.79
7	2.0	5.0	30.0	37.3814	45.2558	-21.07
8	4.0	20.0	30.0	57.1197	51.6646	9.55
9	4.0	12.5	20.0	62.7545	63.1664	-0.66
10	2.0	5.0	20.0	52.8878	52.8158	0.14
11	3.0	5.0	20.0	52.5983	56.6106	-7.63
12	2.0	20.0	20.0	45.0923	51.2516	-13.66
13	2.0	20.0	40.0	37.2452	37.9305	-1.84
14	4.0	5.0	30.0	53.0677	47.9169	9.71
15	2.0	5.0	40.0	33.9726	30.9109	9.01
16	3.0	20.0	20.0	54.5086	57.8063	-6.05
17	4.0	12.5	30.0	51.2703	56.5400	-10.28
18	3.0	12.5	40.0	44.9122	44.3822	1.18
19	2.0	12.5	20.0	72.4874	60.2829	16.84
20	4.0	5.0	40.0	33.6988	33.1096	1.75
21	4.0	20.0	20.0	56.6502	56.8951	-0.43
22	3.0	12.5	20.0	72.0448	63.9577	11.23
23	3.0	5.0	40.0	32.1947	34.2432	-6.36
24	2.0	12.5	40.0	44.3630	41.1699	7.20
25	4.0	12.5	40.0	41.7253	43.1286	-3.36
26	3.0	12.5	30.0	48.6286	57.5624	-18.37
27	4.0	5.0	20.0	52.7020	55.9394	-6.14

Considering the hydrodynamic efficiency results obtained from the numerical simulation, several regression models were constructed, including a linear regression, two factor interaction and a quadratic model. In Table 3, the p-values and R^2 achieved for each of the considered regression models were listed. The p-values show that all the regression models built are significant ones; however, the quadratic regression model has the best

accepted accuracy since almost 74% of the data variability is explained by the model with a p-value associated < 0.05.

Table 3. Statistical parameters of the built regression models

Regression model	p-value	R^2
Linear regression model	0.0001	0.6044
Two factor interaction regression model	0.0021	0.6125
Quadratic regression model	0.0016	0.7359

In turn, Table 4 indicates the results of ANOVA for identifying significant factors. Decision about the significance of a factor or effect is made based on the p-value. According to the results obtained, the factor x_3 and the quadratic term for x_2 are considered as significant factors on the lift-to-drag ratio. Values greater than 0.05 indicate the model terms are not significant. Furthermore, if there are many insignificant model terms (without considering those required supporting hierarchy), model reduction may improve the model. However, by deleting terms that are insignificant, in this case, R^2 of the regression model was reduced. Therefore, in this occasion, any of the model terms were eliminated from the parameter list.

Table 4. ANOVA for the fitted quadratic model using 3^3 full factorial design

Terms	Effect	SS	df	MS	F-ratio	p-value
Model		2218.8	9	246.533	5.26	0.0016
A:Gap, d (x_1)	15.5020	26.3787	1	26.3787	0.56	0.4632
B:Overlap, h (x_2)	2.7551	71.5575	1	71.5575	1.53	0.2332
C:Flap deflection angle, δ (x_3)	0.8934	1724.39	1	1724.39	36.82	0.0000
AA	-2.2329	29.917	1	29.917	0.64	0.4352
AB	-0.0159	0.1728	1	0.1728	0.00	0.9523
AC	0.01861	0.6414	1	0.6414	0.01	0.9082
BB	-0.1199	273.309	1	273.309	5.84	0.0272
BC	0.01861	23.3844	1	23.3844	0.50	0.4894
CC	-0.0339	69.05118	1	69.05118	1.47	0.2412
Error		796.141	17	46.8318		
Total		3014.94	26			

Equation (2) indicates the quadratic regression model fitted to the obtained data. Using this model, the optimal values for x_1 , x_2 and x_3 so that the lift-to-drag ratio is equal to 64.20 are 3.3216%, 12.8145% and 20°, respectively.

$$y = 14.8934 + 15.5020x_1 + 2.7551x_2 + 0.8934x_3 - 0.0159x_1x_2 - 0.0231x_1x_3 + 0.01861x_2x_3 - 2.2329x_1^2 - 0.1199x_2^2 - 0.0339x_3^2 \quad (2)$$

From the regression model, a three-dimensional response surface plot, represented by Figure 2, was generated.

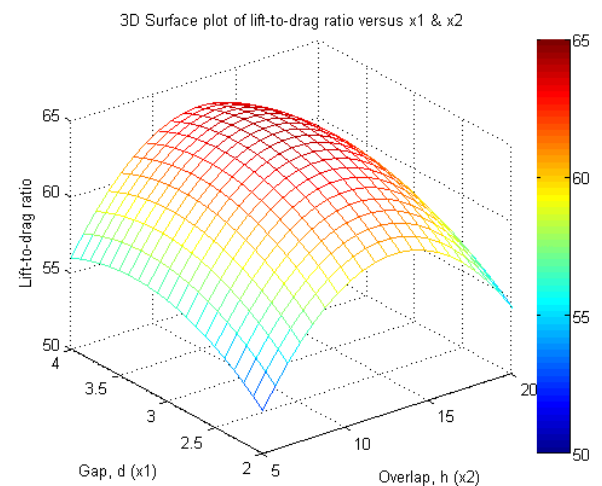


Figure 2. Response surface plot showing the effects of independent variables, gap, d (x_1) and overlap, h (x_2), on the lift-to-drag ratio using 3^3 full factorial design

3.2 Box-Behnken design (BBD)

A 15-run BBD to identify the significant factors for maximizing the lift-to-drag ratio was also conducted. Using the relations listed in Table 1, the actual levels of the variables for each of the numerical studies in the design matrix were calculated. The results obtained from numerical simulation in JavaFoil software are given in Table 5.

Table 5. BBD experimental design matrix and responses

Run	Variables			Lift-to-drag ratio		% Error
	Gap, $d(x_1)$	Overlap, $h(x_2)$	Flap deflection angle, $\delta(x_3)$	Numerical results	Predicted results	
1	2.0	20.0	30.0	56.6672	58.3298	-2.93
2	4.0	12.5	40.0	41.7253	46.8709	-12.33
3	3.0	5.0	40.0	32.1947	28.7118	10.82
4	3.0	12.5	30.0	48.6286	48.6286	0.00
5	2.0	12.5	40.0	44.3630	42.3812	4.47
6	3.0	12.5	30.0	48.6286	48.6286	0.00
7	3.0	5.0	20.0	52.5983	52.6286	-0.06
8	3.0	20.0	40.0	38.4138	38.7329	-0.83
9	3.0	12.5	30.0	48.6286	48.6286	0.00
10	4.0	12.5	20.0	62.7545	64.7363	-3.16
11	3.0	20.0	20.0	54.5086	57.9915	-6.39
12	2.0	12.5	20.0	72.4874	67.3418	7.10
13	2.0	5.0	30.0	37.3814	42.8461	-14.62
14	4.0	20.0	30.0	57.1197	51.6550	9.57
15	4.0	5.0	30.0	53.0677	51.4051	3.13

Several regression models for the response variable were constructed, including a linear, two factor interaction and a quadratic regression model, as observed in Table 6. The adequacy of the models was evaluated by R^2 and p-value. The analysis of the results reveal that the quadratic model has the highest R^2 (0.9007) with a p-value lower than 0.05 (0.0448). The value of R^2 shows that only 9.99% of the total variation of the obtained data could not be explained by the referred regression model. Therefore, it can be concluded that this regression model resulted to be a highly significant model.

Table 6. Statistical parameters of the built regression models

Regression model	p-value	R^2
Linear model	0.0040	0.6875
Two factor interaction model	0.0448	0.7372
Quadratic model	0.0448	0.9007

The equation of the quadratic regression model describing the lift-to-drag ratio is expressed in Equation (3). From Equation (3), predicted values for each combination of the considered levels of the factors are presented in Table 5.

$$y = 123.6540 - 38.5053x_1 + 3.4999x_2 - 1.8045x_3 - 0.5078x_1x_2 + 0.1774x_1x_3 + 0.01436x_2x_3 + 6.6671x_1^2 - 0.01436x_2^2 + 0.0004x_3^2 \quad (3)$$

where y refers to the lift-to-drag ratio, and x_1 , x_2 , and x_3 are the coded levels for the d , h , and δ , respectively.

Table 7. ANOVA for the fitted quadratic model using BBD

Term	Effect	SS	df	MS	F-ratio	p-value
Model		1365.8	9	151.756	5.04	0.0448
A:Gap, $d(x_1)$	-38.5053	1,77492	1	1,77492	0.06	0,8178
B:Overlap, $h(x_2)$	3.4999	123,773	1	123,773	4,11	0,0984
C:Flap deflection angle, $\delta(x_3)$	-1.8045	917,033	1	917,033	30,46	0,0027
AA	6.6671	164,121	1	164,121	5,45	0,0668
AB	-0.5078	58,0172	1	58,0172	1,93	0,2237
AC	0.1774	12,5855	1	12,5855	0,42	0,5464
BB	-0.01436	66,2740	1	66,274	2,20	0,1980
BC	0.01436	4,6414	1	4,64144	0,15	0,7108
CC	0.0004	0,0050	1	0,0050	0,00	0,9902
Error		150,5290	5	30,1059		
Total		1516,330	14			

In Table 7, the results obtained from the ANOVA are compiled. It can be observed that the term x_3 has the highest F-value and the lowest p-value, which means that the settling time has the largest effect on the lift-to-drag ratio. The rest of the model terms have no significant influence on the lift-to-drag ratio. The term CC, related to the quadratic effect of δ , was eliminated from the list of

parameters influencing the system because it was observed to have the highest p-value and higher than 0.05. Following the elimination of this term, R^2 was not modified but the p-value associated with the model decreased to 0.0155, lower than 0.0448. Therefore, by eliminating insignificant terms the significance of the regression model increased.

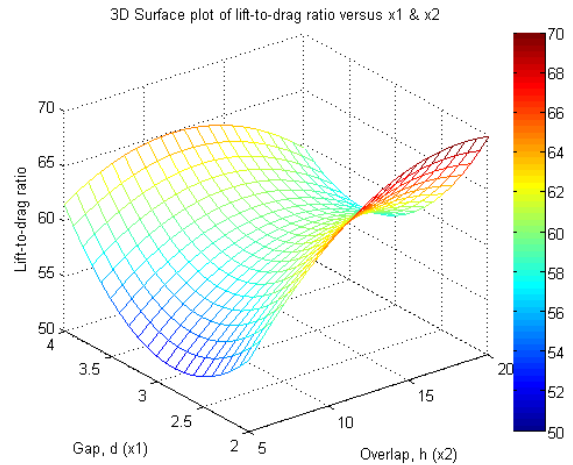


Figure 3. Response surface plot showing the effects of independent variables, gap, $d(x_1)$ and overlap, $h(x_2)$, on the lift-to-drag ratio using BBD

Once the regression model is constructed, the optimal value for the lift-to-drag ratio was calculated resulting to be 69.9626 when $d(x_1)$; $h(x_2)$; and $\delta(x_3)$ were equal to 2.0%, 18.4619% and 20°, respectively. The response surface obtained can be found in Figure 3.

3.3 Central composite design (CCD)

CCD corresponds to first-order (2^k) designs augmented by additional center and axial points to allow estimation of the tuning parameters of a second-order model [15]. In this study, the CCD created was composed of a 2^3 DOE plus star points, studying the effects of 3 factors in 16 runs, as observed in Table 8. It is important to note that the design was run in a single block and the order of the experiments was fully randomized. This kind of DOE presents an alternative DOE to 3^k design in the construction of regression models and finding the optimal conditions for a particular process, since using CCD the number of experiments is reduced, as compared to a full factorial DOE (16 in the case of CCD compared to 27 for a full factorial design). Consequently, the saving in operating costs when finding the optimal domain for a process to be operated or manufactured is substantially high.

Table 8. CCD experimental design matrix and responses

Run	Variables			Lift-to-drag ratio		% Error
	Gap, $d(x_1)$	Overlap, $h(x_2)$	Flap deflection angle, $\delta(x_3)$	Numerical results	Predicted results	
1	3.0	12.5	30.0	48.6286	54.9636	-13.03
2	2.0	5.0	40.0	33.9726	34.8062	-2.45
3	2.0	20.0	20.0	45.0923	47.8801	-6.18
4	3.0	12.5	40.0	44.9122	46.2583	-3.00
5	4.0	5.0	40.0	33.6988	32.4948	-3.57
6	2.0	5.0	20.0	52.8878	53.5548	-1.26
7	4.0	20.0	20.0	56.6502	57.4004	-1.32
8	4.0	20.0	40.0	39.0216	39.9383	-2.35
9	3.0	5.0	30.0	57.1184	53.3456	6.61
10	2.0	20.0	40.0	37.2452	35.3528	5.08
11	2.0	12.5	30.0	46.1229	43.7269	5.19
12	3.0	12.5	20.0	72.0448	64.3637	10.66
13	3.0	20.0	30.0	56.7923	54.2300	4.51
14	4.0	5.0	20.0	52.7020	56.1782	-6.60
15	4.0	12.5	30.0	51.2703	47.3313	7.68
16	3.0	12.5	30.0	48.6286	54.9636	-13.03

The numerical results were fitted by multiple linear regression using a linear model, two factor interaction model and quadratic model. Table 9 contains the p-values and R^2 of the regression

models used. From the table, the highest R^2 found is linked to the quadratic regression model. Although the p-value associated to the regression model is higher than 0.05, its value is close to 0.05. In this regard, it can be concluded that the best regression models among the regression model constructed using CCD for the maximization of the lift-to-drag ratio response variable was the quadratic regression model.

Table 9. Statistical parameters of the built regression models

Regression model	p-value	R^2
Lineal regression model	0.0138	0.5750
Two factor interaction regression model	0.1182	0.6122
Quadratic regression model	0.0518	0.8582

The estimated effects of each operating variable and the ANOVA results for the quadratic regression model are presented in Table 10. The interaction effect between δ (C) term and the quadratic term referred to h (BB) term on the lift-to-drag ratio was found to be significant. The other model terms had no significant influence on the lift-to-drag ratio. From the quadratic regression model, the term related to the quadratic effect for δ (CC) was eliminated from the parameter list because it has the highest p-value and it is higher than 0.05. When this term was eliminated, R^2 still adopted an acceptable value equal to 0.85801 with an associated p-value lower than 0.05. Deleting the rest of the insignificant terms resulted in a reduction of R^2 . Therefore, any model term was additionally removed from the parameter list. If CC term is eliminated, the final equation in terms of coded factors was given as expressed by Equation (4).

Table 10. ANOVA for the fitted quadratic model using CCD

Terms	Effect	SS	df	MS	F-ratio	p-value
Model with CC		1274.61	9	141.623	4.04	0.0518
Model without CC		1274.29	8	159.286	5.29	0.0204
A:Gap, $d(x_1)$	59.2367	32.4796	1	32.4796	0.93	0.3732
B:Overlap, $h(x_2)$	-0.7303	1.9554	1	1.9554	0.06	0.8212
C:Flap deflection angle, $\delta(x_3)$	-1.0028	819.508	1	819.508	23.35	0.0029
AA	-9.4345	234.663	1	234.663	10.31	0.0184
AB	0.2299	23.7840	1	23.7840	0.68	0.4419
AC	-0.1234	12.1759	1	12.1759	0.35	0.5773
BB	-0.0209	3.6446	1	3.6446	0.09	0.7685
BC	0.0207	19.3526	1	19.3526	0.55	0.4858
CC	0.0035	0.3181	1	0.3181	0.01	0.9272
Error		210.562	6	35.0936		
Total		1485.17	15			

$$y = -5.5234 + 58.5735x_1 - 0.7794x_2 - 0.7944x_3 + 0.2299x_1x_2 - 0.1234x_1x_3 + 0.0207x_2x_3 - 9.324x_1^2 - 0.01894x_2^2 \quad (4)$$

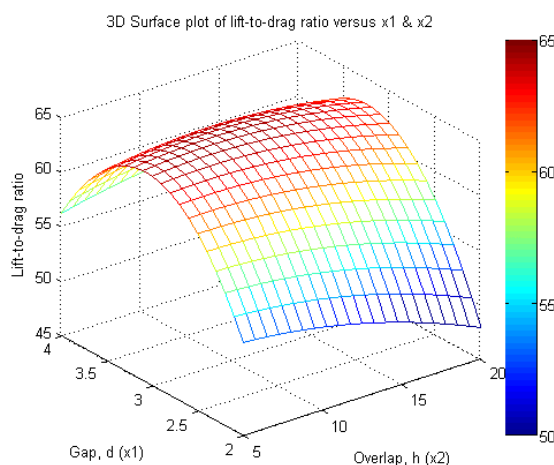


Figure 4. Response surface plot showing the effects of independent variables, gap, $d(x_1)$ and overlap, $h(x_2)$, on the lift-to-drag ratio using CCD

Using this model, the optimal value of 64.52 for the lift-to-drag ratio is achieved when the factors x_1 , x_2 and x_3 are equal to 3.1237%, 9.3329% and 20° , respectively. This can be observed in Figure 4, representing the response surface for the lift-to-drag ratio under the experimental domain.

3.4 Comparing DOE for the second order linear regression model

For all the obtained DOE, the factor resulting with the highest effect on the response variable was δ , represented by x_3 . For the studied DOE, the optimal value of the referred factor was 20° . However, it is important to note that DOE methods are used to significantly reduce the amount of time and computational effort consumed in analyzing the effect of varying factors affecting a model and analyzing their effect on a response [15], [16]. Using DOE, the runs are structured in such a way that the effects of the main factors and the two-way interactions between factors are considered [15]-[16]. In DOE, representing the relation between independent variables and response variables is possible by constructing an effective response surface. The determination of the optimal values or operating conditions for the parameters included in the models can be achieved through regression analysis techniques [15]-[18].

It is highlighted that the full factorial design is usually considered impractical, due to the excessive number of experiments (or simulations) needed to construct the relationship between the responses (function values) and factors (independent variables) by regression analyses. Therefore, other DOE such as BBD and CCD are preferred since a reduced number of runs are required and the number of runs becomes prevalent in the practice when higher-order interactions of the factors can be ignored [15]. Adding runs to DOE do not always lead to a rise in R^2 . This reduction in runs results in lower costs. From the obtained results, the best R^2 was obtained through the BBD with 15 runs. Additionally, the regression model obtained from BBD allowed for the highest lift-to-drag ratio with a p-value lower than 0.05 by using only 15 runs. Through this DOE, the optimal values for x_1 , x_2 and x_3 factors were 2.0%, 18.4619% and 20° , respectively. Under this treatment, the maximal lift-to-drag ratio was 69.9626.

3.5 Verification of the regression model assumptions

There are several assumptions that must be checked (among them the assumption of normality; *i.e.*, the data obtained following a normal distribution), because the validity of the obtained regression model depends on this aspect.

Normality can be assessed graphically, by constructing both a frequency distribution and a normal probability plot for the obtained data, where data following a normal distribution are adjusted to the represented line [15]. In Figure 5, both frequency distribution (Figure 5a) and normal probability plot (Figure 5b) for the lift-to-drag ratio are illustrated. In the figure, it is not clear if normality is achieved, since in Figure 5a data do not exactly follow the line representing a normal distribution. Additionally, in Figure 5b some of the data seem to be away from the straight line, which refers to normality. Although visual inspection of the distribution might be used for assessing normality, this approach is usually unreliable and does not guarantee that the data distribution is normal. Therefore, numerical tests must be performed [15]. The main tests for the assessment of normality are Kolmogorov-Smirnov test (including Limiting form, Stephens methods, Marsaglia method and Lilliefors test), Shapiro-Wilk test, Shapiro-Francia test, Anderson-Darling test, Cramer-von Mises test, D'Agostino and Pearson test, and Jarque-Bera test.

The results of the normality tests showed that the lift-to-drag ratio followed a normal distribution. In addition to normality verification, homoscedasticity, linearity and residual independency were checked. It was achieved that the regression model built through BBD can be used to explain the simulated data found.

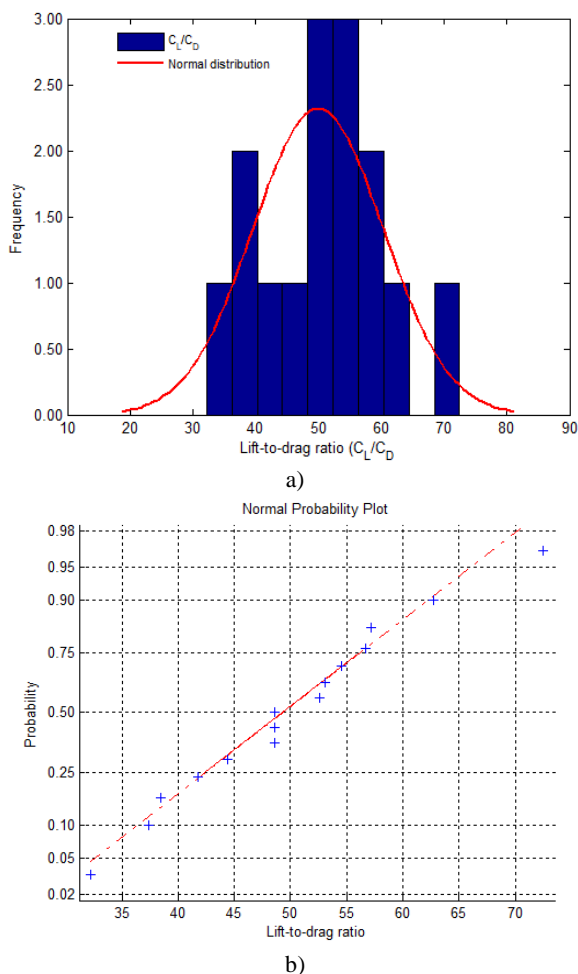


Figure 5. a) Histogram and b) Normal probability plot for the lift-to-drag ratio response variable using BBD

4. Conclusion

RSM is a useful and powerful tool to provide a prediction model representing the lift-to-drag ratio, as well as the optimal conditions of the factors influencing the performance of a multi-element hydrofoil, in order to achieve the highest possible performance. In the current work, several DOE, including a 3^k full factorial design, BBD and CCD were conducted to obtain the optimal values for d , h and δ . It was found that by using BBD the maximal lift-to-drag ratio was 69.9626. This value was achieved under d , h and δ equal to 2.0%, 18.4619% and 20° , respectively. Additionally, it was found that the lift-to-drag ratio is strongly affected by the variations of δ .

Acknowledgement

The authors gratefully acknowledge the financial support provided by the Colombia Scientific Program within the framework of the call Ecosistema Científico (Contract No. FP44842-218-2018).

References

[1] M. Anyi and B. Kirke, "Evaluation of small axial ow hydrokinetic turbines for remote communities", in *Energy for Sustainable Development*, 2010, Vol. 14 (2), pp.110-116.

[2] D. Kumar and S. Sarkar, "A review on the technology, performance, design optimization, reliability, techno-economics and environmental impacts of hydrokinetic energy conversion

systems", in *Renewable and Sustainable Energy Reviews*, 2016, Vol. 58, pp. 796-813.

[3] H.J. Vermaak, K. Kusakana and S.P. Koko, "Status of micro-hydrokinetic river technology in rural applications: A review of literature", in *Renewable and Sustainable Energy Reviews*, 2014, Vol. 29, pp. 625-633.

[4] N. Kolekar, S. Mukherji, and A. Banerjee, "Numerical Modeling and Optimization of Hydrokinetic Turbine", in *ASME. Energy Sustainability, ASME 2011 5th International Conference on Energy Sustainability, Parts A, B, and C*, pp. 1211-1218.

[5] D.U. Kuma, S. Kannan, D. Vimal Chand, R. Sriram and C. Ganapathi, "Aerodynamic Analysis of Multi Element Airfoil", in *Journal of Aeronautics and Aerospace Engineering*, 2016, Vol. 5, pp. 171.

[6] Y. Tahir, K. Birol, A. Hursit, E. Özgür, "Performance Analysis of a Hydrofoil with and without Leading Edge Slat", in *10th International Conference on Machine Learning and Applications and Workshops*, 2011.

[7] T. Yavuz and E. Koç, "Performance analysis of double blade airfoil for hydrokinetic turbine applications", in *Energy Conversion and Management*, 2012, Vol. 63, pp. 95-100.

[8] S. Narsipur, B.W. Pomeroy and M.S. Selig, "CFD Analysis of Multielement Airfoils for Wind Turbines", in *30th AIAA Applied Aerodynamics Conference 25-28 June 2012, New Orleans, Louisiana*, pp. 2012-2781.

[9] F. Zahle, M. Gaunaa, N.N. Sørensen and C. Bak, "Design and Wind Tunnel Testing of a Thick, MultiElement High-Lift Airfoil", in *Proceedings of EWEA 2012 - European Wind Energy Conference & Exhibition European Wind Energy Association (EWEA)*.

[10] A.M. Ragheb and M.S. Selig, "Multi-Element Airfoil Configurations for Wind Turbines", in *29th AIAA Applied Aerodynamics Conference 27 - 30 June 2011, Honolulu, Hawaii*. AIAA 2011-3971.

[11] J.Y. Li, R. Li, Y. Gao, J. Huang, "Aerodynamic optimization of wind turbine airfoils using response surface techniques", in *Proceedings of the Institution of Mechanical Engineering, Part A: Journal of Power and Energy*, 2010, Vol. 224, pp. 827-838.

[12] A.C. Benim, M. Diederich, B. Pfeiffelmann, "Aerodynamic optimization of airfoil profiles for small horizontal axis wind turbines", in *Computation*, 2018, Vol. 6, pp. 34-53.

[13] H. Sun, "Wind turbine airfoil design using response surface method", in *Journal of Mechanical Science and Technology*, 2011, Vol. 25(5), pp. 1135-1340.

[14] A. Chehouri, R. Younes, A. Ilinca and J. Perron, "Review of performance optimization techniques applied to wind turbines", in *Applied Energy*, 2015, Vol. 142, pp. 361-388.

[15] R.H. Myers, D.C. Montgomery and C.M. Anderson-Cook, "Response Surface Methodology: Process and Product Optimization Using Designed Experiments", in 4th ed.; Wiley: Hoboken, NJ, USA, 2016.

[16] M.D. Manshadi and M. Jamalinasab, "Optimizing a two-element wing model with morphing flap by means of the response surface method", in *Iranian Journal of Science and Technology: Transitions of Mechanical Engineering*, 2017, Vol. 41, pp. 343-352.

[17] A.I. Khuri and S. Mukhopadhyay, "Response Surface Methodology", in *WIREs Computational Statistics*, 2010, Vol. 2, pp. 128-149.

[18] M. Cavazzuti, "Design of Experiments", in *Optimization Methods*. Springer, Berlin, Heidelberg, 2013, pp. 13-42.